BIOCHEMISTRY
including biophysical chemistry & molecular biology

ARTICLE

pubs.acs.org/biochemistry

Variations in Filament Conformation Dictate Seeding Barrier between Three- and Four-Repeat Tau

Paul D. Dinkel,[†] Ayisha Siddiqua,[†] Huy Huynh, Monil Shah, and Martin Margittai*

Department of Chemistry and Biochemistry, University of Denver, Denver, Colorado 80208, United States

Supporting Information

ABSTRACT: Tau filaments are the pathological hallmark of >20 neurodegenerative diseases including Alzheimer's disease. Six tau isoforms exist that can be grouped into 4-repeat (4R) tau and 3-repeat (3R) tau based on the presence or absence of the second of four microtubule binding repeats. Recent evidence suggests that tau filaments can transfer between cells and spread through the brain. Here we demonstrate in vitro that seeded filament growth, a prerequisite for tau spreading, is crucially dependent on the isoform composition of individual seeds. Seeds of 3R tau and 3R/4R tau recruit both types of isoforms. Seeds of 4R tau recruit 4R tau, but not 3R tau, establishing an asymmetric barrier. Conformational templating of 4R tau onto 3R tau seeds eliminates this barrier, giving rise to a new type of tau filament. These findings provide fundamental mechanistic insights into the seeding, propagation, and diversification of tau filaments.

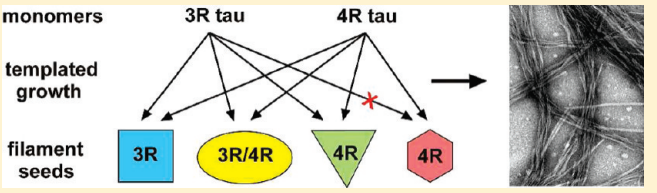

The intracellular deposition of filamentous tau is a common feature of numerous fatal neurodegenerative diseases including Alzheimer's disease, Pick's disease, and progressive supranuclear palsy.[1] Through transcription from a single gene and alternative mRNA splicing six different tau isoforms are produced, ranging in size from 352 to 441 amino acids. The isoforms can be divided into two major groups: (1) 4R tau, which contains 4 microtubule binding repeats (each 31−32 amino acids long), and (2) 3R tau, which contains 3 microtubule binding repeats (lacking repeat 2) (Figure 1A). In the adult human brain 3R and 4R tau coexist at equimolar ratios.[2] This ratio is reflected in the tau proteins found in the filamentous inclusions of Alzheimer's disease.[3] In contrast, filaments in progressive supranuclear palsy contain only 4R tau and filaments in Pick's disease contain only 3R tau.[4] The molecular basis for the differences in tau deposition is not understood.

Soluble tau is an intrinsically disordered protein with a net positive charge and a low tendency to aggregate.[5] The addition of negatively charged cofactors such as heparin greatly accelerates aggregation.[6] Upon fibrillization the repeat region becomes structured, forming a protease resistant core.[7,8] The regions flanking the filament core form a fuzzy coat that remains largely unfolded.[9] In tau monomers these regions are thought to fold back onto the repeats.[10] Removal of the flanking regions, as exemplified by the constructs K18 and K19 (Figure 1B), further accelerates aggregation.[5] The assembly of tau monomers into filaments results in the formation of cross-β structure,[11,12] a defining architectural feature of all fibrils belonging to the amyloid class.[13] Tau filament formation (as that of other amyloid fibrils) depends on the assembly of a critical nucleus onto which individual monomers can grow.[14] This event marks the rate-limiting step of aggregation and can be circumvented by the addition of filament seeds.[14−16] Recent experiments have demonstrated that tau filaments can transfer among neighboring cells in tissue culture[17] and that insoluble tau aggregates can spread from the site of injection in mouse brain.[18] Together, these properties are reminiscent of prions[19] and have raised the question of whether prionlike mechanisms might be responsible for tau pathogenesis.[20,21] Prion diseases, unlike tauopathies, are infectious.[22] However, infectivity and interneuronal transmissibility of prions are thought to be based on a single molecular principle: recruitment of monomeric proteins onto the fibril ends.[23] Understanding this recruitment process for tau may provide important molecular insights into the interneuronal spreading of tauopathies.

We have recently demonstrated that based on composition three distinct types of tau filaments exist: (1) 3R tau, (2) 4R tau, and (3) 3R/4R.[24] Here we have used these filaments to investigate tau-seeded fibrillization. Our findings show important mechanistic parallels to prions that could help explain phenotypic variations in human tauopathies.

EXPERIMENTAL PROCEDURES

Plasmid Constructs. All constructs used in this study have been described previously.[24] Briefly, K18 and K19 were cloned into pET28b via the NcoI/XhoI cleavage sites. Natural cysteines (1 in K19 and 2 in K18) were replaced by serines. These constructs and their corresponding proteins are referred to as "cysteine-free". Single cysteines were subsequently introduced by site-directed mutagenesis using the QuikChange method from Stratagene/Agilent Technologies.

Received: March 28, 2011
Revised: April 21, 2011
Published: April 21, 2011

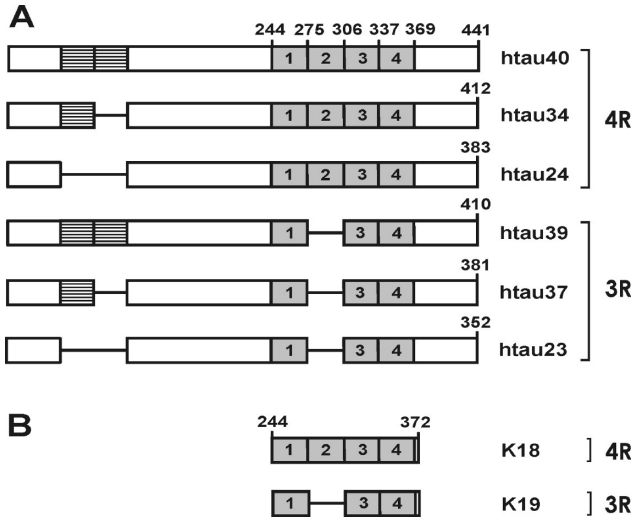

Figure 1. Tau isoforms and constructs. (A) Tau isoforms are defined by the presence or absence of two inserts (striped) in the N-terminal half and the inclusion or exclusion of the second microtubule binding repeat (marked as 2) in the C-terminal half. (B) The constructs K18 and K19 encompass the repeat region. 4R = 4-repeat, 3R = 3-repeat.

Protein Expression and Purification. All tau proteins were expressed and purified as previously described,[24] exploiting their heat stability and high isoelectric points. In brief, *Escherichia coli* bacteria (strain BL21(DE3)) with overexpressed tau proteins were pelleted by centrifugation and resuspended in extraction buffer (500 mM NaCl, 20 mM Pipes, pH 6.5, 1 mM EDTA, 50 mM 2-mercaptoethanol). After storage at −80 °C, bacteria were heated for 20 min at 80 °C and further treated by sonification. Soluble tau protein was separated from bacterial debris after 15 min centrifugation at 15 000*g*. Precipitation of tau occurred by the addition of 60% (mass per volume) ammonium sulfate. After 1 h incubation at 25 °C, each protein sample was sedimented for 15 min at 15000*g*, resolubilized in dH_2O (2 mM DTT), passed through a syringe filter and applied onto a MonoS cation exchange column (GE Healthcare). Tau protein was eluted from the column by a NaCl gradient. Enriched fractions, as judged by SDS PAGE, were pooled and further purified via passage over a Superdex 200 gelfiltration column. All K18 and K19 constructs were precipitated overnight with a 3-fold volumetric excess of acetone. In all cases, 2.5 mM DTT was present during precipitation to avoid oxidation damage. Subsequently, proteins were pelleted by centrifugation, aliquoted, and washed with acetone in the presence of 2 mM DTT. All proteins were stored at −80 °C until further use.

Acrylodan Labeling. Single cysteine mutants of tau (4−6 mg) were taken up in 8 M guanidine hydrochloride and labeled for 1 h with a ∼10-fold molar excess of acrylodan (Invitrogen). In order to remove denaturant and excess dye, each protein sample was passed over a PD-10 desalting column from GE Healthcare. Cysteine-free proteins were treated the same way, except that no label was added after uptake in guanidine hydrochloride. All protein concentrations were determined by the BCA method (Pierce).

Seed Production. 25 μM of cysteine-free K18 and K19 (or a combination of 12.5 μM K18 and 12.5 μM K19) were mixed with 50 μM heparin (average molecular mass of 5000 Da, Celsus, Cincinnati, OH) and allowed to grow under agitation for 3 days at 25 °C. Subsequently, the filaments (500 μL) were sonified for 20 s at power setting 3 in a Fisher Scientific Sonifier (150 Series). Seed morphology was verified by negative stain electron microscopy. Reactions that involved multiple cycles of seeding and elongation were sonified after 1 h incubation.

Seeding Assay and Fluorescence Detection. All reactions were performed in 100 mM NaCl, 10 mM Hepes, pH 7.4. The following mole percentages were used for all reactions: 2% acrylodan-labeled tau, 98% cysteine-free tau. The final concentration of monomeric proteins K18 and K19 was 10 μM. Also present was a 2-fold molar excess of heparin to tau. Seeding reactions were initiated by the addition of 3 mol % seeds. Experiments that involved multiple cycles of seeding and elongation contained higher concentrations of monomers (25 μM) and larger mole percentages of seeds (8%). These increases were performed to accelerate aggregation. After 1 h, each reaction was sonified to produce seeds for the next reaction cycle. The final seeding step in this multicycle procedure contained 3 mol % seeds and 10 μM monomers. All reactions were monitored in a Fluorolog 3 system (Horriba, Jobin). Temperatures were set at 37 °C using a solid state Pelletier element. Excitation occurred at 360 nm. Single emission spectra ranging from 400 to 600 nm were collected with excitation and emission slit widths set at 5 nm.

Negative Stain Electron Microscopy (EM). 250-mesh carbon coated copper grids were placed for 40 s onto 10 μL drops of tau filaments (10 μM) for 30 s on 10 μL drops of 2% uranyl acetate and subsequently air-dried on filter paper. All images were taken with a Philips/FEI Tecnai-12 electron transmission microscope at 80 keV and equipped with a Gatan CCD camera.

RESULTS

Seeds of 3R/4R Tau Nucleate the Formation of 3R and 4R Tau Filaments. We have previously shown that upon mixing monomers of 3R and 4R tau do not segregate into separate aggregates, but instead coassemble into heterogeneous filaments.[24] 3R and 4R tau incorporate into these filaments with similar probability and distribute evenly over the length of the fiber.[24] Whether the filaments can effectively seed the propagation of individual 3R and 4R tau monomers is not known. In order to address this question, we used the environment sensitive dye acrylodan[25] to monitor the recruitment of monomeric tau into the filaments. Specifically, acrylodan was cross-linked to a single cysteine (Figure 2A) at position 310 in the third repeat of K19. This site was chosen as it is located in the core of the filament[24,26] and as such undergoes large conformational changes upon aggregation. Furthermore, spin-labeling of the site had no measurable effect on overall structure.[24] Cross-linking with acrylodan resulted in a new side chain, henceforth referred to as A1. In preparation for filament formation, the labeled protein was mixed with a 50-fold molar excess of cysteine-free K19. Upon excitation at 360 nm, the emission spectrum revealed a maximum at 523 nm (Figure 2B), characteristic for an aqueous solvent exposed site.[27] This result is in good agreement with tau being intrinsically disordered.[28,29] The addition of seeds (produced through ultrasonic shearing of K18/K19 filaments) initiated aggregation. Upon completion, the spectrum had blue-shifted to a new emission maximum at 462 nm (Figure 2B), indicating label exposure to a more hydrophobic environment.[27] The shift in the inverse emission wavelength was plotted as a function of time revealing the elongation kinetics

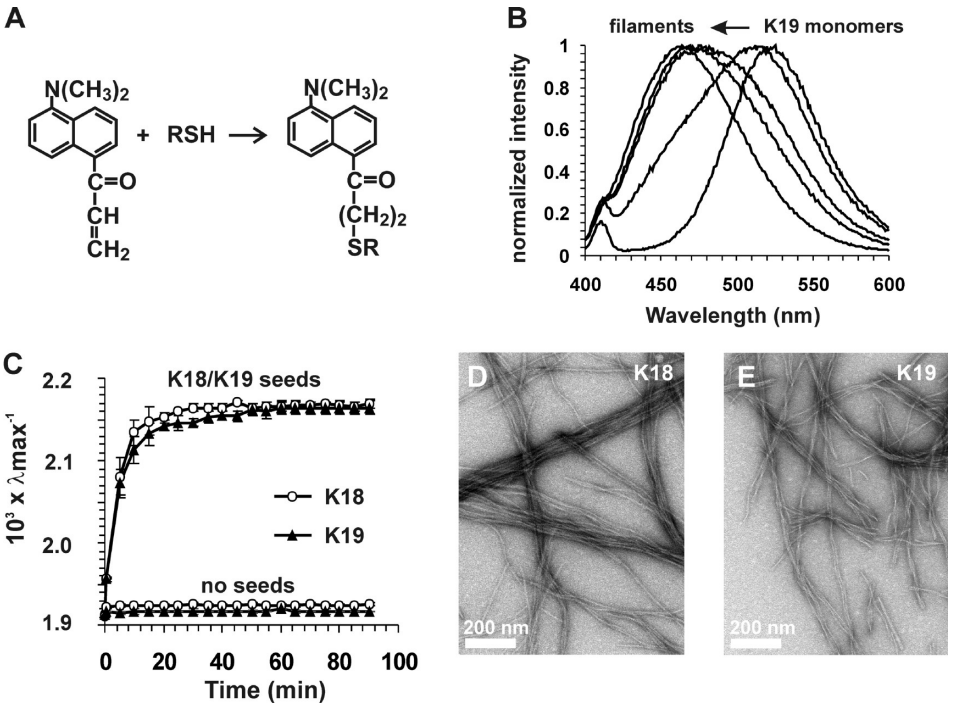

Figure 2. Seeds of K18/K19 effectively template growth of K18 and K19. (A) Scheme for acrylodan labeling of cysteine side chain. (B) Addition of 3% K18/K19 seeds to a mixture of monomers of 98% K19 and 2% K19_310A1 (total concentration: 10 μM) results in a time-dependent blue shift in the emission maximum. Traces from right to left represent reactions after 0, 0.5, 5, 10, and 80 min. Excitation: 360 nm; emission: 400−600 nm. (C) The inverse wavelength plotted as a function of time reveals the progression of K19 (closed triangles) and K18 (open circles) aggregation. In the absence of seeds no changes are observed. Values represent mean ±s.d. (n = 3 experiments). (D, E) Electron micrographs of K18 and K19 filaments produced through K18/K19-seeded reactions.

of K19 (Figure 2C). In a next step an equivalent set of measurements was carried out for K18. The same seeds produced similar elongation kinetics (Figure 2C). In the absence of seeds, neither K18 nor K19 aggregated (Figure 2C). The presence of filaments in the seeded reactions was confirmed by negative stain electron microscopy (Figure 2D,E). Together, these findings reveal that filaments of 3R/4R tau serve as seeds for the formation of 3R and 4R tau filaments.

Cross-Seeding Barrier Prevents Growth of 3R Tau onto 4R Tau Seeds. K18 and K19 differ by the inclusion or exclusion of the second microtubule binding repeat (Figure 1B). To determine whether this variation in sequence affects filament conformation, we tested the seeding properties of K18 and K19 filaments. In a first set of experiments, we prepared seeds from K18 filaments and monitored the elongation of K18 and K19 monomers onto these seeds. As before, acrylodan was cross-linked to position 310 and served to report filament growth. Again, a 50-fold molar excess of the respective cysteine-free construct was mixed into each reaction. While K18 monomers grew onto K18 seeds, K19 monomers did not (Figure 3A). Importantly, a 3- or 5-fold increase in seed concentration did not lead to any measurable incorporation of K19 monomers (Figure S1A), indicating a robust conformational barrier. The inability of K19 monomers to grow onto K18 seeds did not originate from acrylodan labeling at position 310, as monomers labeled in different positions (317, 322) failed to integrate as well (Figure S1B). Electron micrographs confirmed this seeding behavior as filaments were observed for K18 (Figure 3B), but not for K19 (Figure 3C). In a next step we produced seeds from K19 filaments. To our surprise both K18 and K19 monomers added onto these seeds (Figure 3D). However, the addition of K19 monomers was markedly more efficient. The filamentous nature of the aggregates was confirmed by electron microscopy (Figure 3E,F). In order to independently verify the seeding properties of K18 and K19 filaments, we repeated all experiments using an extrinsic thioflavin T based assay (Figure S1C,D). The same asymmetric barrier was observed. Furthermore, replacement of the truncated monomers with full-length versions of tau (htau23 and htau40) produced similar seeding characteristics, albeit with slower kinetics (Figure S1E,F). Combined, these data suggest that conformational differences between filaments of 3R and 4R tau allow growth of 4R tau onto 3R tau seeds but prevent growth of 3R tau onto 4R tau seeds.

Cross-Seeding Gives Rise to a New Type of 4R Tau Filament. The observation that 4R tau can grow onto 3R tau seeds raised the question of whether the resulting filaments have the ability to seed 3R tau. Such a property would be expected if the monomers of 4R tau assumed the conformation of the seeds of 3R tau. In order to address this question, we carried out a three step seeding experiment (Figure 4A). In the first step K18 monomers were grown onto K19 seeds. In the second step three cycles of seeding and elongation produced an enriched population of K18 filaments. In the third step seeds of these K18 filaments were added to K19 monomers. Remarkably, the K18 seeds had the ability to seed the formation of K19 filaments (Figure 4B, top trace). As a result of the multistep procedure the concentration of K19 seeds was reduced from 2.0×10^{-6} M in the first reaction to 3.1×10^{-11} M in the final reaction. At this final seed concentration K19 does not accelerate aggregation (not shown), and therefore the growth of K19 monomer was not

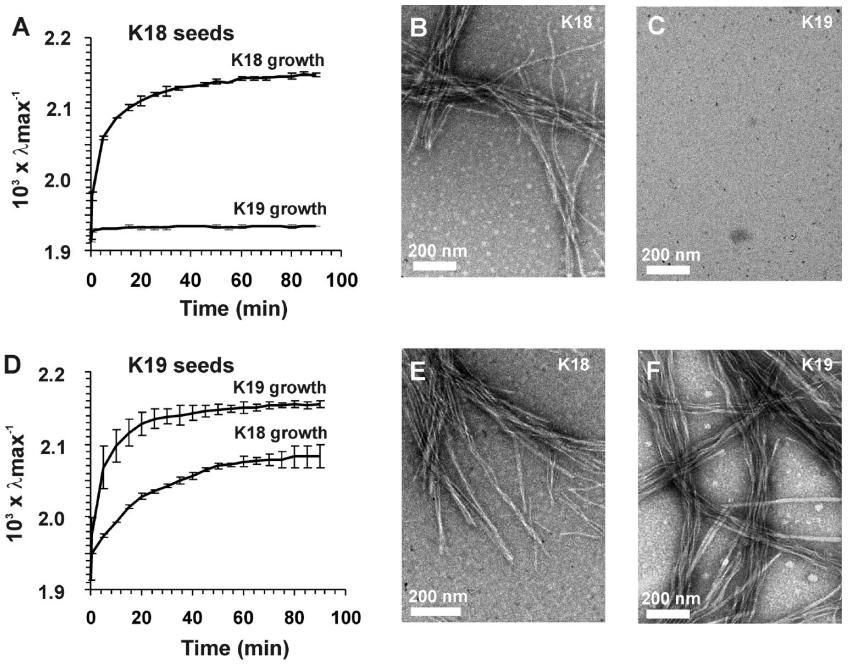

Figure 3. Asymmetric barrier for K18 and K19 cross-seeding. (A) Aggregation of K18 monomers (98% K18, 2% K18_310A1) and K19 monomers (98% K19, 2% K19_310A1) in the presence of 3% K18 seeds. (B) Electron micrograph of K18 filaments seeded with K18. (C) Electron micrograph of K19 grown onto K18 seeds. (D) Aggregation of K19 monomers (98% K19, 2% K19_310A1) and K18 monomers (98% K18, 2% K18_310A1) in the presence of 3% K19 seeds. (E) Electron micrograph of K18 grown onto K19 seeds. (F) Electron micrograph of K19 grown onto K19 seeds. Protein concentrations were 10 μM. All values represent mean ± s.d. (n = 3 experiments).

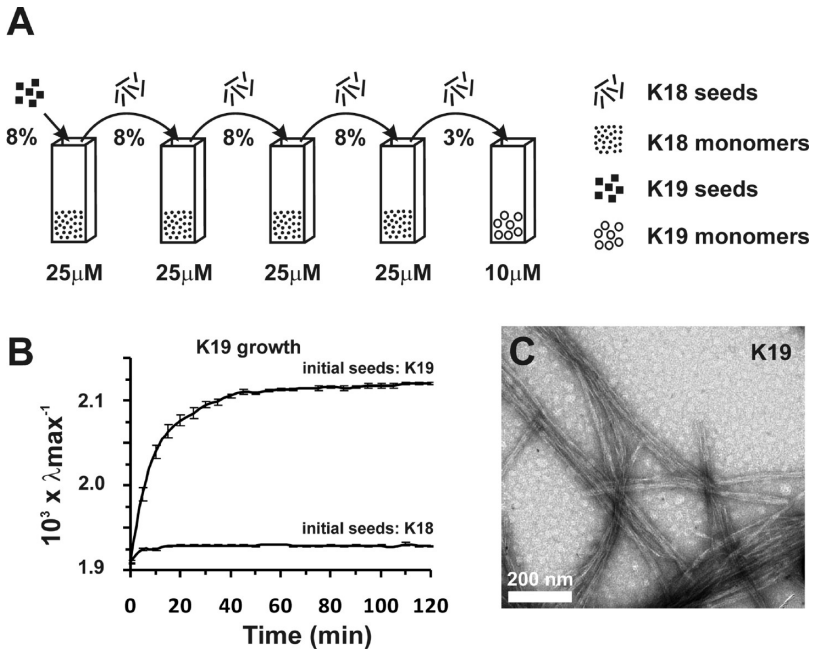

Figure 4. Tau filament diversification. (A) Experimental design of multicycle seeding reactions. (B) Aggregation of K19 monomers (98% K19, 2% K19_310A1) in the presence of 3% K18 seeds (last step in A) monitored as a change in inverse emission wavelength over time (top trace). When instead of K19 seeds K18 seeds were present in the initial seeding step, no aggregation occurred (bottom trace). (C) Electron micrograph representing the end point of the top trace in (B).

affected by any residual K19 seeds. The presence of filaments was visually confirmed by EM (Figure 4C). Importantly, when the initial seeds in the multistep seeding procedure were composed of K18, seeding of K19 in the final step did not occur (Figure 4B, bottom trace). Corresponding results were obtained when full-length tau was used in the final elongation step (Figure S2A,B). These observations are important as they demonstrate that the same protein, K18, can produce filaments with different

dx.doi.org/10.1021/bi2004685 |*Biochemistry* 2011, 50, 4330–4336

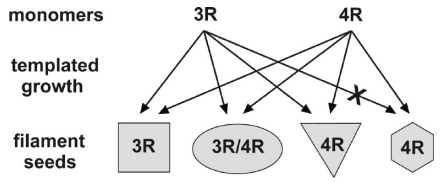

Figure 5. Templated filament growth of tau. Monomers of 3R and 4R tau (top) can only grow onto the ends of 3R (square), 3R/4R (oval), and 4R filaments (triangle and hexagon) if their sequence is compatible with the conformation of the seed (arrows). Structural incompatibility gives rise to a seeding barrier (crossed out arrow).

seeding properties, depending on the initial template, and furthermore that these properties can be propagated over multiple generations.

DISCUSSION

The identification of three compositionally distinct types of tau filaments that share a common core with parallel, in-register arrangement of β-strands[24,30,31] has raised the question of whether these filaments could be conformationally distinct. Variations in packing interactions could impart different biophysical properties. Here, we set out to identify such differences between the three types of filaments by investigating their seeding characteristics. Recent evidence suggests that caspase-cleaved fragments,[32] and other truncated forms of tau,[33] may play a critical role in the initiation of filament formation. These smaller forms show greatly accelerated kinetics and seeds thereof may serve as templates onto which full-length isoforms bind.[32,33] For seeds, we chose the constructs K18 and K19, which are truncated versions of tau that contain the core-forming repeat region (Figure 1B). We made following key observations irrespective of whether truncated (K18 and K19) or full-length versions of tau (htau23 and htau40) were used for filament growth (summarized in Figure 5): First, seeds of 3R tau and 3R/4R tau recruit both types of isoforms. Second, seeds of 4R tau recruit 4R tau, but not 3R tau, establishing an asymmetric barrier. Third, conformational templating of 4R tau onto 3R tau seeds abolishes this barrier giving rise to a new type of tau filament. These results indicate the existence of at least four conformationally distinct types of filaments.

Conformationally distinct fibrils are a hallmark of prions and are thought to be the basis for strain (or phenotype) variations in mammals[34,35] and yeast.[36,37] Strain identity is thought to be maintained by imprinting the conformation of the prion fibril onto the soluble prion proteins via seeded conversion.[38,39] Prion proteins that vary in sequence may also be recruited giving rise to the transmission of prions from one species to another or, in the case of polymorphisms, the transmission within species.[23] This processs can lead to the emergence of new strains as exemplified by the appearance of variant Creutzfeld Jacob's disease, which has been linked to the transmission of bovine prions to humans.[40] If the primary structure of the variant is incompatible with the conformation of the seed, a transmission barrier occurs. The seeding barrier that prohibits 3R tau from growing onto 4R tau seeds is reminiscent of such a barrier, suggesting that the primary structure of 3R tau is incompatible with the conformation of 4R tau seeds. The primary structure of 4R tau, however, is compatible with the conformation of 3R tau seeds, leading to the emergence of a new type of filament. A similar asymmetry in seeding specificity observed for 3R and 4R tau has been described for the tau disease mutant P301L.[41] While seeds of this mutant recruited its respective monomers, wild type monomers were not recruited. Wild type seeds, on the other hand, were able to recruit both mutant and wild type tau. Whether P301L that had been grown onto the wild type seeds resembled a new type of filament that was able to seed wild type tau had not been addressed. Regardless, these findings demonstrate that the coexistence of different tau isoforms and the presence of tau mutants could have intricate effects on the propagation.

On the basis of their seeding properties, we have identified four conformationally distinct types of filaments (Figure 5). It is likely that additional types of filaments exist. Previous experiments have demonstrated that 4R tau can adopt different conformations when grown onto distinct seeds,[42] revealing a structural plasticity of tau akin to that of other amyloid proteins (see for example refs 35, 36, and 43−45). The in vitro conditions that are used for filament formation arguably do not recapitulate the complex biochemical environment in the human brain. Cofactors, chaperones, and post-translational modifications could affect filament formation in a cell-dependent manner. In fact, in the case of prions it has been shown that different cell lines can favor different prion strains[46] and that selective pressures can cause the amplification of new strains and the disappearance of old ones.[47] Despite their deficiencies, our in vitro experiments have demonstrated that tau filaments have the ability to seed, propagate, and diversify and that conformational barriers can determine isoform recruitment. Our experiments suggest that the initial nucleation event may have a profound effect on subsequent filament formation. Nuclei that contain 3R and 4R tau could establish templates that recruit all isoforms. Such a type of recruitment could be important in Alzheimer's disease where all isoforms are deposited.[3] Nuclei that contain only 4R tau could establish templates that recruit only 4R tau. Importantly, such a conformational barrier could explain the preferential deposition of 4R tau in progressive supranuclear palsy, corticobasal degeneration, and other 4R tauopathies. Although our in vitro experiments do not explain the preferential deposition of 3R tau in Pick's disease, it is possible that inefficient growth of 4R tau onto 3R tau seeds leaves these filaments prone to cellular clearance. Alternatively, an additional type of 3R tau filament may exist that is conformationally incompatible with 4R tau. Despite this lack of understanding, the molecular mechanisms that explain strain diversity, transmission barriers, and strain emergence in prion diseases are clearly inherent in tau, suggesting that similar phenomena might exist in tauopathies.

ASSOCIATED CONTENT

Supporting Information. Independent data confirming asymmetric seeding barrier between 3R and 4R tau (Figure S1) and data corroborating filament diversification of 4R tau (Figure S2). This material is available free of charge via the Internet at http://pubs.acs.org.

AUTHOR INFORMATION

Corresponding Author

*Tel: (303) 871-4135. Fax: (303) 871-2254. E-mail: martin.margittai@du.edu.

Author Contributions

†These authors contributed equally.

Funding Sources

This work was supported by grants from CurePSP — Society for Progressive Supranuclear Palsy (M.M.).

■ ACKNOWLEDGMENT

We are grateful for access to the electron microscopy core facility at the University of Colorado Health Sciences Center.

■ ABBREVIATIONS

3R, 3-repeat; 4R, 4-repeat; aa, amino acid; EDTA, ethylenediaminetetraacidic acid; DTT, dithiothreitol.

■ REFERENCES

(1) Lee, V. M., Goedert, M., and Trojanowski, J. Q. (2001) Neurodegenerative tauopathies. *Annu. Rev. Neurosci. 24*, 1121–1159.

(2) Goedert, M., Spillantini, M. G., Jakes, R., Rutherford, D., and Crowther, R. A. (1989) Multiple isoforms of human microtubule-associated protein tau: sequences and localization in neurofibrillary tangles of Alzheimer's disease. *Neuron 3*, 519–526.

(3) Goedert, M., Spillantini, M. G., Cairns, N. J., and Crowther, R. A. (1992) Tau proteins of Alzheimer paired helical filaments: abnormal phosphorylation of all six brain isoforms. *Neuron 8*, 159–168.

(4) Buee, L., and Delacourte, A. (1999) Comparative biochemistry of tau in progressive supranuclear palsy, corticobasal degeneration, FTDP-17 and Pick's disease. *Brain Pathol. 9*, 681–693.

(5) Barghorn, S., and Mandelkow, E. (2002) Toward a unified scheme for the aggregation of tau into Alzheimer paired helical filaments. *Biochemistry 41*, 14885–14896.

(6) Goedert, M., Jakes, R., Spillantini, M. G., Hasegawa, M., Smith, M. J., and Crowther, R. A. (1996) Assembly of microtubule-associated protein tau into Alzheimer-like filaments induced by sulphated glycosaminoglycans. *Nature 383*, 550–553.

(7) Wischik, C. M., Novak, M., Thogersen, H. C., Edwards, P. C., Runswick, M. J., Jakes, R., Walker, J. E., Milstein, C., Roth, M., and Klug, A. (1988) Isolation of a fragment of tau derived from the core of the paired helical filament of Alzheimer disease. *Proc. Natl. Acad. Sci. U.S.A. 85*, 4506–4510.

(8) Novak, M., Kabat, J., and Wischik, C. M. (1993) Molecular characterization of the minimal protease resistant tau unit of the Alzheimer's disease paired helical filament. *EMBO J. 12*, 365–370.

(9) Wischik, C. M., Novak, M., Edwards, P. C., Klug, A., Tichelaar, W., and Crowther, R. A. (1988) Structural characterization of the core of the paired helical filament of Alzheimer disease. *Proc. Natl. Acad. Sci. U.S.A. 85*, 4884–4888.

(10) Jeganathan, S., von Bergen, M., Brutlach, H., Steinhoff, H. J., and Mandelkow, E. (2006) Global hairpin folding of tau in solution. *Biochemistry 45*, 2283–2293.

(11) von Bergen, M., Barghorn, S., Li, L., Marx, A., Biernat, J., Mandelkow, E. M., and Mandelkow, E. (2001) Mutations of tau protein in frontotemporal dementia promote aggregation of paired helical filaments by enhancing local beta-structure. *J. Biol. Chem. 276*, 48165–48174.

(12) Berriman, J., Serpell, L. C., Oberg, K. A., Fink, A. L., Goedert, M., and Crowther, R. A. (2003) Tau filaments from human brain and from in vitro assembly of recombinant protein show cross-beta structure. *Proc. Natl. Acad. Sci. U.S.A. 100*, 9034–9038.

(13) Sunde, M., and Blake, C. (1997) The structure of amyloid fibrils by electron microscopy and X-ray diffraction. *Adv. Protein Chem. 50*, 123–159.

(14) Friedhoff, P., von Bergen, M., Mandelkow, E. M., Davies, P., and Mandelkow, E. (1998) A nucleated assembly mechanism of Alzheimer paired helical filaments. *Proc. Natl. Acad. Sci. U.S.A. 95*, 15712–15717.

(15) Nonaka, T., Watanabe, S. T., Iwatsubo, T., and Hasegawa, M. (2010) Seeded aggregation and toxicity of {alpha}-synuclein and tau: cellular models of neurodegenerative diseases. *J. Biol. Chem. 285*, 34885–34898.

(16) Guo, J. L., and Lee, V. M. (2011) Seeding of normal tau by pathological tau conformers drives pathogenesis of Alzheimer-like tangles. *J. Biol. Chem. 286*, 15317−15331.

(17) Frost, B., Jacks, R. L., and Diamond, M. I. (2009) Propagation of tau misfolding from the outside to the inside of a cell. *J. Biol. Chem. 284*, 12845–12852.

(18) Clavaguera, F., Bolmont, T., Crowther, R. A., Abramowski, D., Frank, S., Probst, A., Fraser, G., Stalder, A. K., Beibel, M., Staufenbiel, M., Jucker, M., Goedert, M., and Tolnay, M. (2009) Transmission and spreading of tauopathy in transgenic mouse brain. *Nat. Cell Biol. 11*, 909–913.

(19) Prusiner, S. B. (1998) Prions. *Proc. Natl. Acad. Sci. U.S.A. 95*, 13363–13383.

(20) Goedert, M., Clavaguera, F., and Tolnay, M. (2010) The propagation of prion-like protein inclusions in neurodegenerative diseases. *Trends Neurosci. 33*, 317–325.

(21) Frost, B., and Diamond, M. I. (2010) Prion-like mechanisms in neurodegenerative diseases. *Nat. Rev. Neurosci. 11*, 155–159.

(22) Collinge, J. (2001) Prion diseases of humans and animals: their causes and molecular basis. *Annu. Rev. Neurosci. 24*, 519–550.

(23) Collinge, J., and Clarke, A. R. (2007) A general model of prion strains and their pathogenicity. *Science 318*, 930–936.

(24) Siddiqua, A., and Margittai, M. (2010) Three- and four-repeat Tau coassemble into heterogeneous filaments: an implication for Alzheimer disease. *J. Biol. Chem. 285*, 37920–37926.

(25) Prendergast, F. G., Meyer, M., Carlson, G. L., Iida, S., and Potter, J. D. (1983) Synthesis, spectral properties, and use of 6-acryloyl-2-dimethylaminonaphthalene (Acrylodan). A thiol-selective, polarity-sensitive fluorescent probe. *J. Biol. Chem. 258*, 7541–7544.

(26) Andronesi, O. C., von Bergen, M., Biernat, J., Seidel, K., Griesinger, C., Mandelkow, E., and Baldus, M. (2008) Characterization of Alzheimer's-like paired helical filaments from the core domain of tau protein using solid-state NMR spectroscopy. *J. Am. Chem. Soc. 130*, 5922–5928.

(27) Wearsch, P. A., Voglino, L., and Nicchitta, C. V. (1998) Structural transitions accompanying the activation of peptide binding to the endoplasmic reticulum Hsp90 chaperone GRP94. *Biochemistry 37*, 5709–5719.

(28) Cleveland, D. W., Hwo, S. Y., and Kirschner, M. W. (1977) Physical and chemical properties of purified tau factor and the role of tau in microtubule assembly. *J. Mol. Biol. 116*, 227–247.

(29) Schweers, O., Schonbrunn-Hanebeck, E., Marx, A., and Mandelkow, E. (1994) Structural studies of tau protein and Alzheimer paired helical filaments show no evidence for beta-structure. *J. Biol. Chem. 269*, 24290–24297.

(30) Margittai, M., and Langen, R. (2006) Side chain-dependent stacking modulates tau filament structure. *J. Biol. Chem. 281*, 37820–37827.

(31) Margittai, M., and Langen, R. (2004) Template-assisted filament growth by parallel stacking of tau. *Proc. Natl. Acad. Sci. U.S.A. 101*, 10278–10283.

(32) de Calignon, A., Fox, L. M., Pitstick, R., Carlson, G. A., Bacskai, B. J., Spires-Jones, T. L., and Hyman, B. T. (2010) Caspase activation precedes and leads to tangles. *Nature 464*, 1201–1204.

(33) Wang, Y. P., Biernat, J., Pickhardt, M., Mandelkow, E., and Mandelkow, E. M. (2007) Stepwise proteolysis liberates tau fragments that nucleate the Alzheimer-like aggregation of full-length tau in a neuronal cell model. *Proc. Natl. Acad. Sci. U.S.A. 104*, 10252–10257.

(34) Legname, G., Nguyen, H. O., Peretz, D., Cohen, F. E., DeArmond, S. J., and Prusiner, S. B. (2006) Continuum of prion protein structures enciphers a multitude of prion isolate-specified phenotypes. *Proc. Natl. Acad. Sci. U.S.A. 103*, 19105–19110.

(35) Colby, D. W., Giles, K., Legname, G., Wille, H., Baskakov, I. V., DeArmond, S. J., and Prusiner, S. B. (2009) Design and construction of diverse mammalian prion strains. *Proc. Natl. Acad. Sci. U.S.A. 106*, 20417–20422.

(36) Tanaka, M., Chien, P., Naber, N., Cooke, R., and Weissman, J. S. (2004) Conformational variations in an infectious protein determine prion strain differences. *Nature 428*, 323–328.

(37) King, C. Y., and Diaz-Avalos, R. (2004) Protein-only transmission of three yeast prion strains. *Nature 428*, 319–323.

(38) Jones, E. M., and Surewicz, W. K. (2005) Fibril conformation as the basis of species- and strain-dependent seeding specificity of mammalian prion amyloids. *Cell 121*, 63–72.

(39) Castilla, J., Morales, R., Saa, P., Barria, M., Gambetti, P., and Soto, C. (2008) Cell-free propagation of prion strains. *EMBO J. 27*, 2557–2566.

(40) Collinge, J., Sidle, K. C., Meads, J., Ironside, J., and Hill, A. F. (1996) Molecular analysis of prion strain variation and the aetiology of 'new variant' CJD. *Nature 383*, 685–690.

(41) Aoyagi, H., Hasegawa, M., and Tamaoka, A. (2007) Fibrillogenic nuclei composed of P301L mutant tau induce elongation of P301L tau but not wild-type tau. *J. Biol. Chem. 282*, 20309–20318.

(42) Frost, B., Ollesch, J., Wille, H., and Diamond, M. I. (2009) Conformational diversity of wild-type Tau fibrils specified by templated conformation change. *J. Biol. Chem. 284*, 3546–3551.

(43) Petkova, A. T., Leapman, R. D., Guo, Z., Yau, W. M., Mattson, M. P., and Tycko, R. (2005) Self-propagating, molecular-level polymorphism in Alzheimer's beta-amyloid fibrils. *Science 307*, 262–265.

(44) Paravastu, A. K., Qahwash, I., Leapman, R. D., Meredith, S. C., and Tycko, R. (2009) Seeded growth of beta-amyloid fibrils from Alzheimer's brain-derived fibrils produces a distinct fibril structure. *Proc. Natl. Acad. Sci. U.S.A. 106*, 7443–7448.

(45) Kodali, R., Williams, A. D., Chemuru, S., and Wetzel, R. (2010) Abeta(1−40) forms five distinct amyloid structures whose beta-sheet contents and fibril stabilities are correlated. *J. Mol. Biol. 401*, 503–517.

(46) Mahal, S. P., Baker, C. A., Demczyk, C. A., Smith, E. W., Julius, C., and Weissmann, C. (2007) Prion strain discrimination in cell culture: the cell panel assay. *Proc. Natl. Acad. Sci. U.S.A. 104*, 20908–20913.

(47) Li, J., Browning, S., Mahal, S. P., Oelschlegel, A. M., and Weissmann, C. (2010) Darwinian evolution of prions in cell culture. *Science 327*, 869–872.